JOURNAL OF GEOPHYSICAL RESEARCH, VOL. 96, NO. A2, PAGES 1439–1449, FEBRUARY 1, 1991

A Particle Simulation of Large-Amplitude Undulations on the Evening Diffuse Auroral Boundary

TAKASHI YAMAMOTO

Geophysics Research Laboratory, University of Tokyo

K. MAKITA

Department of Engineering, Takushoku University, Tokyo

C.-I. MENG

Applied Physics Laboratory, The Johns Hopkins University, Laurel, Maryland

The pattern of undulation on the equatorward boundary of the diffuse aurora, occasionally observed in the afternoon-evening sector, is studied by two-dimensional particle simulations for the motion of magnetospheric plasma perpendicular to the geomagnetic field. In the simulation model, the poleward electric field is assumed to be initially enhanced locally in latitude and independent of longitude, as suggested by the observations near the undulations of the diffuse auroral boundary. Such an electric field is assumed to be maintained by space charges carried by a cold plasma. The diffuse aurora is initially distributed over a longitudinally extended zone. Since this type of diffuse aurora is probably caused by precipitation of the energetic protons with energies in excess of a few keV, the temporal evolution of the diffuse auroral pattern, as displayed in photographs from the satellites, can be visualized by following the cluster of the energetic protons. Sheared plasma flow arising from the electric field distribution drives the Kelvin-Helmholtz instability and causes undulations on the equatorward boundary of the diffuse aurora with wavelengths and amplitudes comparable to the typical observed values. Notably, the particle simulation can reproduce the outstanding indentations characteristic of large-amplitude undulations which have occasionally been observed. The good agreement between the simulation results and the observed undulations suggests that the Kelvin-Helmholtz shear-driven process is responsible for undulations on the equatorward boundary of the diffuse aurora in the afternoon-evening sector. It is also shown that the magnetic drift of the energetic protons producing the diffuse aurora is important in creating the characteristic pattern of the diffuse auroral boundary.

1. INTRODUCTION

It has been shown by numerical simulations that the Kelvin-Helmholtz (K-H) instability plays an important role in auroral arc dynamics. *Miura and Sato* [1978] demonstrated that the growth of K-H waves leads to curl-type distortions similar to those observed in the aurora [*Hallinan and Davis*, 1970; *Oguti*, 1974]. A more systematic analysis of the deformations of curls and folds was carried out by *Wagner et al.* [1983]. They showed that curls form when the sheath thickness of hot ions is large in comparison with the electron sheet. Folds can occur when the ion sheath is thin, i.e., the ratio of ion to electron temperature is near unity. Recently, considerable progress has been achieved in the theoretical analysis of the K-H instability and associated phenomena in magnetospheric and ionospheric plasmas. *Lyons and Walterscheid* [1985] suggested a possible connection between a K-H instability of the neutral winds and the generation of auroral omega bands. Effects of finite Larmor radius on the K-H instability were discussed by *Pritchett and Coroniti* [1984] and *Pritchett* [1987]. Effects of electron dynamics along the magnetic field and Coulomb collisions on this instability were examined by *Satyanarayana et al.* [1987]. *Keskinen et al.* [1988] presented numerical simulations of the development of K-H waves with ionospheric Pedersen conductivity coupling. *Ganguli et al.* [1988] and *Nishikawa et al.* [1988] discussed a kinetic ion cyclotron instability driven by a localized electric field perpendicular to an ambient magnetic field.

Using photographs from the Defense Meteorological Satellite Program (DMSP) satellite, *Lui et al.* [1982] first reported occurrences of large-amplitude undulations on the equatorward boundary of the diffuse aurora in the afternoon-evening sector. The crest-to-trough amplitude of these waveforms ranges from about 40 to 400 km, and the wavelength varies from about 200 to 900 km. Auroral images from successive DMSP passes suggest that this phenomenon lasts for about 0.5–3.5 hours. In all cases observed, the undulations occur during a geomagnetic storm interval near the peak development of the storm time ring current.

Several satellite experiments have shown the existence of large localized meridional electric fields, or, equivalently, sheared azimuthal flow near the equatorward boundary of the diffuse aurora (for a brief review, see *Kelley* [1986]). This fact suggests that the diffuse auroral undulations are caused by an instability of this sheared flow. (Lui et al. first suggested the Kelvin-Helmholtz instability as one possible mechanism for the undulations.) Recently, *Kelley* [1986] conducted a search for near-simultaneous data from satellite

Paper number 90JA01984.
0148-0227/91/90JA-01984$05.00

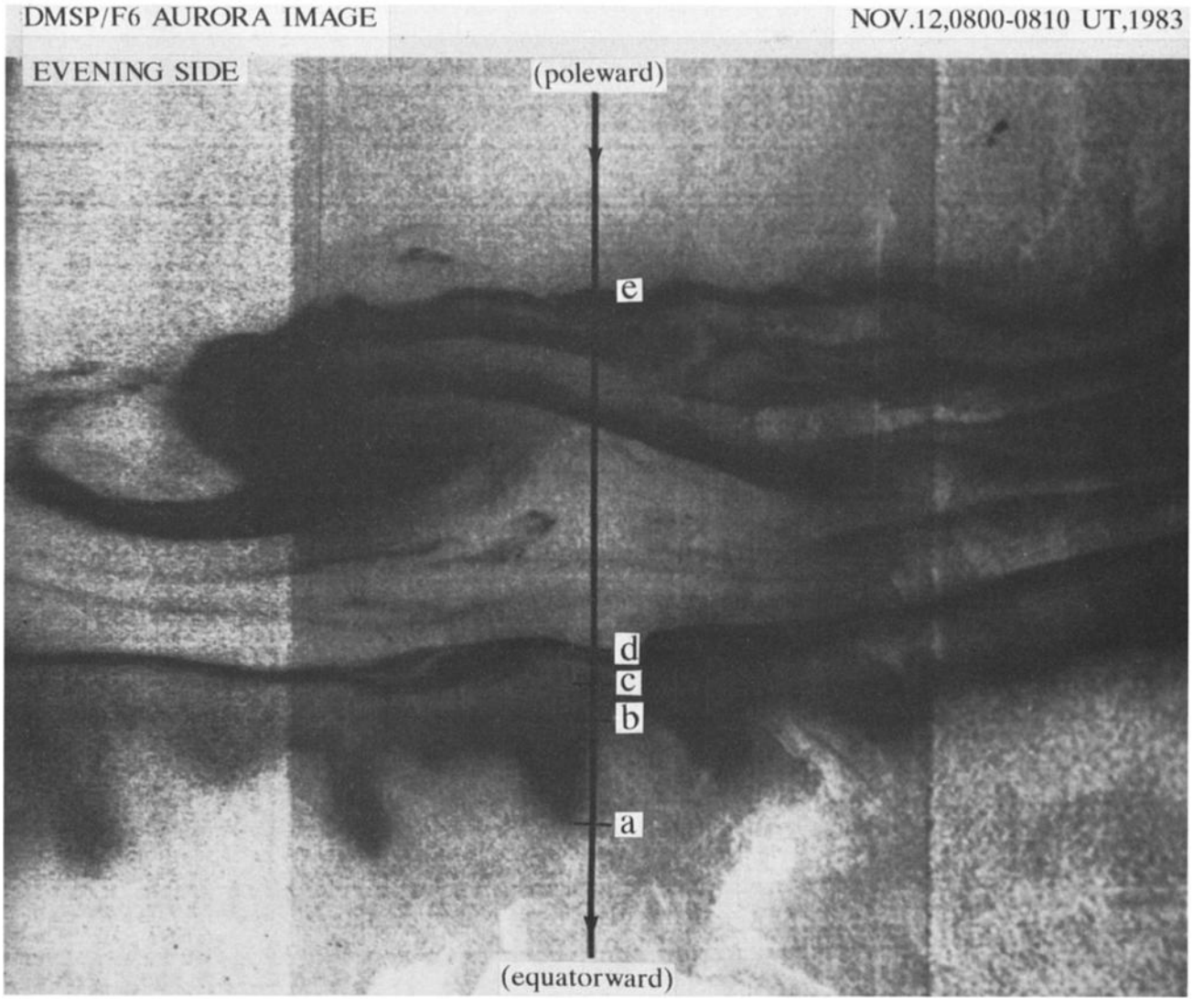

Fig. 1*a*. Undulation on the equatorward boundary of the diffuse aurora in the premidnight sector photographed by the DMSP F6 satellite on November 12, 1983, in the northern hemisphere. A westward traveling surge can also be seen at higher latitudes.

electric field receivers and from DMSP photographs of the undulations. The closest example was a satellite pass indicating shear 20 min after a DMSP photograph showed strong undulations which had been developing for at least 1 hour. On the basis of a theory by *Viñas and Madden* [1986], Kelley argued that several of the undulation events satisfied the magnetic Richardson number criterion for instability and that the observed wavelengths are in good agreement with the theory. So far, however, theoretical work has never demonstrated the development of large-amplitude undulations on the equatorward boundary of diffuse aurora in a synthetic system which includes diffuse auroral particles as well as space charges responsible for the localized meridional electric fields. Note that the undulation pattern of the diffuse aurora occasionally exhibits remarkable indentations as seen in DMSP photographs (see Figure 1*a*). It may therefore be a challenging problem for computational physics to reproduce such a spectacular pattern in a model magnetosphere and to bring out nonlinear plasma dynamics possibly involved in it. The westward traveling surge that can be seen in Figure 1 has also been simulated numerically

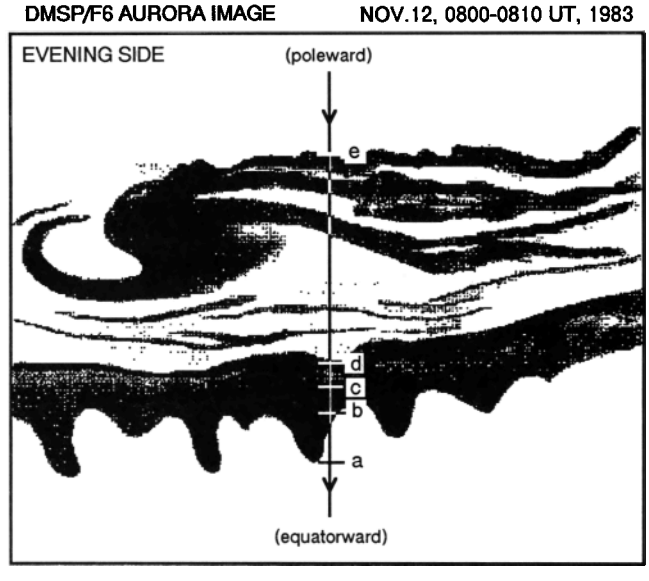

Fig. 1*b*. Sketch of the main auroral features seen in Figure 1*a*.

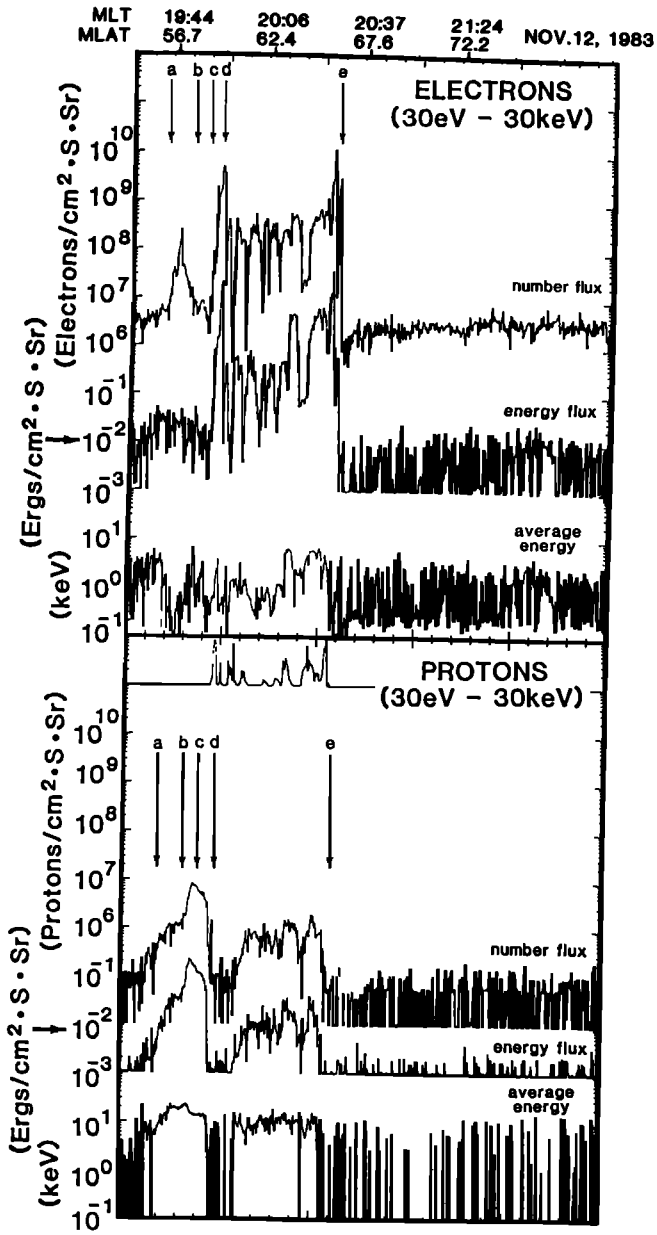

Fig. 1c. Electron and proton precipitation profiles measured along the subtrack as the satellite crossed the auroras in Figure 1a. Labels a–e indicate the positions a–e on the subtrack in the DMSP photograph (Figure 1a). Number fluxes, energy fluxes, and average energies of the precipitated electrons (in the upper panel) and protons (in the lower panel) are shown.

by T. Yamamoto et al. (A particle simulation of the westward traveling surge, submitted to *Journal of Geophysical Research*, 1990).

The purpose of the present paper is to show that large-amplitude undulations observed on the equatorward boundary of diffuse aurora can be identified with spatial modulation of magnetically drifting auroral protons by the electrostatic Kelvin-Helmholtz instability due to the sheared azimuthal flow. By performing two-dimensional particle simulations we obtain the indentation pattern of the energetic proton cluster, which is quite similar to the large-amplitude undulations observed.

2. Basic Equations

To begin, we present the basic equations which primarily govern the plasma electrostatic dynamics in a plane perpendicular to the magnetic field. If a velocity shear is present across the geomagnetic field over a distance much larger than the ion Larmor radius, the electrostatic shear instability takes place in a frequency regime below the ion cyclotron frequency [*Miura and Sato*, 1978]. This may be the case in a region magnetically connected to the diffuse aurora of interest. We are then allowed to use the guiding center drift approximation. The electron and ion guiding center velocities $\mathbf{V}_e$ and $\mathbf{V}_i$ are expressed as

$$\mathbf{V}_e = \mathbf{V}_E + \mathbf{V}_G + \mathbf{V}_C = \mathbf{E} \times \mathbf{B}/B^2 - (W_{\perp e}/e)\mathbf{B} \times \nabla B/B^3 - (2W_{\parallel e}/e)\mathbf{B} \times (\hat{b} \cdot \nabla)\hat{b}/B^2 \quad (1)$$

$$\mathbf{V}_i = \mathbf{V}_E + \mathbf{V}_G + \mathbf{V}_C = \mathbf{E} \times \mathbf{B}/B^2 + (W_{\perp i}/e)\mathbf{B} \times \nabla B/B^3 + (2W_{\parallel i}/e)\mathbf{B} \times (\hat{b} \cdot \nabla)\hat{b}/B^2 \quad (2)$$

where $\mathbf{E}$ is the electric field arising from charge separation; $\mathbf{B}$ is the geomagnetic field; $\hat{b}$ is the unit vector parallel to $\mathbf{B}$, i.e., $\hat{b} = \mathbf{B}/B$; e is the electronic charge; $W_\perp$ and $W_\parallel$ are the perpendicular and parallel kinetic energies, respectively, of a particle; and the subscripts e and i denote the electron and ion species, respectively. The second and third terms in each equation represent the gradient-B and curvature drifts while the polarization drift is neglected.

In our two-dimensional model, it is assumed that the plasma is composed of a uniform equilibrium part with density n_0 and a nonuniform perturbed part which is related to the charge separation. Expressing the electron and ion number densities as $n_e = n_0 + \delta n_e$ and $n_i = n_0 + \delta n_i$, the Poisson's equation is then written as

$$\text{div } \mathbf{E} = -\nabla^2\phi = (e/\varepsilon_0)(\delta n_i - \delta n_e)$$

where ϕ is the electrostatic potential, i.e., $\mathbf{E} = -\nabla\phi$, and ε_0 is the dielectric constant of free space. Thus we need to solve only for the perpendicular (to $\mathbf{B}$) motion of plasma particles constituting the nonuniform part when an initial distribution of these particles is given [*Yamamoto and Yamashita*, 1988].

3. Simulation Model

In this section we present a simulation model to study the temporal and spatial development of the diffuse aurora involved in an electrostatic shear instability in the magnetosphere. Since the electrostatic acceleration of diffuse auroral particles parallel to the magnetic field is negligible, the geomagnetic field lines are nearly equipotential in the diffuse auroral region. Therefore it suffices to consider only the potential distribution at a given altitude. In the present analysis the simulation plane is set at the ionospheric altitude (see Figure 2). Numerical simulations are performed in a rectangular domain on the ionospheric plane covering $0 < x < L_x = 768$ km and $0 < y < L_y = 1536$ km, where the latitudinal coordinate x and longitudinal coordinate y are in units of kilometers and positive directions are poleward and westward, respectively. The z axis is in the direction opposite to the geomagnetic field B. In these Cartesian coordi-

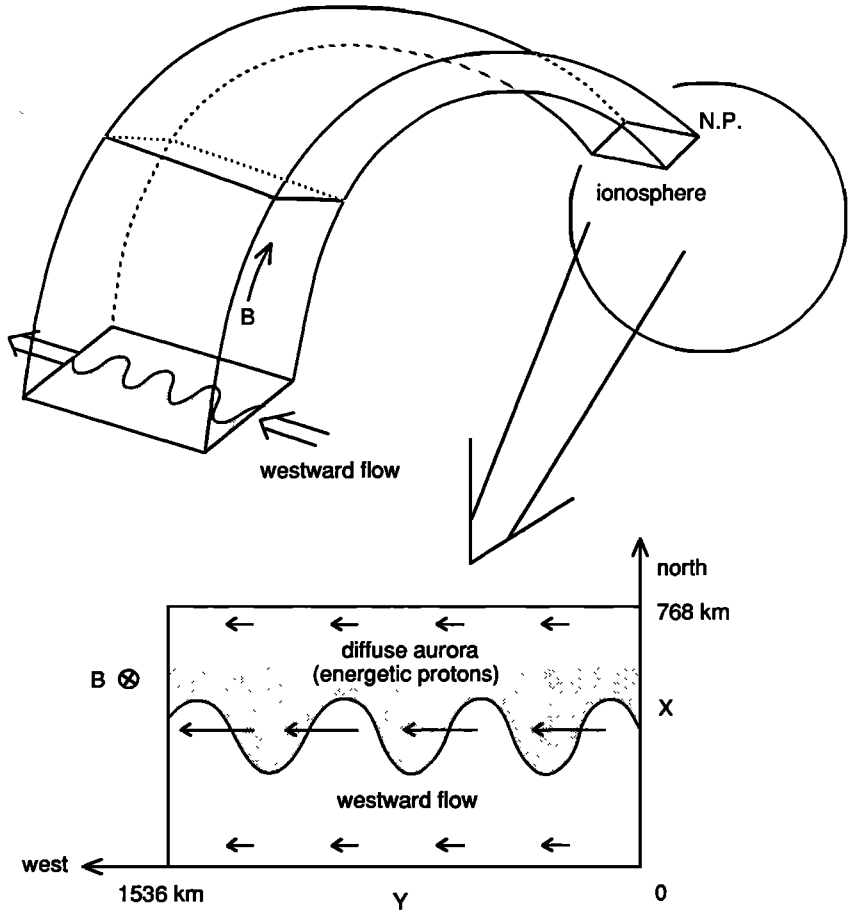

Fig. 2. Schematic illustrating a model system for numerical simulations of undulations on the equatorward boundary of the diffuse aurora. The undulations are identified with spatial modulations of energetic protons by the Kelvin-Helmholtz instability, which is driven by a velocity shear in the westward convection flow. Diffuse auroral undulations are simulated on the ionospheric plane perpendicular to the geomagnetic field. The directions of the x and y axes of an ionospheric coordinate system referred to in the text are indicated.

nates, for simplicity, the x and y directions are identified with the latitudinal and longitudinal directions, respectively.

In the simulation model, initially, the cold plasma flow is assumed to have only a westward (y) component $U(x)$ independent of y, i.e., $\partial U/\partial y = 0$, but a velocity shear of $\partial U/\partial x \neq 0$. The distribution of $U(x)$ is specified as shown in Figure 3*a*. The corresponding distribution of the electrostatic potential is also shown in Figure 3*b*, where the geomagnetic field B is assumed constant in calculating the potential from the plasma flow. Note that the equipotential contours indicate the streamlines of the cold plasma flow V_E. Such a local enhancement of the westward convection flow at the equatorward edge of the auroral oval has been observed by *Smiddy et al.* [1977], *Maynard* [1978], *Spiro et al.* [1979], *Rich et al.* [1980], *Unwin and Cummack* [1980], *Gonzales et al.* [1983], and *Kelley* [1986].

Space charges from the cold plasma are thought to be responsible for the observed sheared plasma flows. In the present model, the local enhancement of the meridional electric field corresponding to the initial flow pattern $U(x)$ is self-consistently formed by two longitudinally elongated strips of cold electrons at high latitude and cold protons at low latitude. The electron and proton strips are centered at x = 417 km and x = 351 km, respectively, and have a latitudinal width of 60 km. The background cold plasma is treated as a uniform incompressible neutral fluid. The particle density in the strips is adjusted so that the maximum flow speed (in $U(x)$) at the ionospheric height is about 3.8 km/s. This is comparable with the peak flow speeds which are deduced from the S3-2 satellite data taken almost simultaneously with occurrences of the diffuse auroral undulations [*Kelley*, 1986]. Also, note the similarity of the flow pattern $U(x)$ in the model and those observed in Figure 4 of *Kelley* [1986]. The diffuse aurora subject to undulations on its equatorward boundary in the afternoon-evening sector may be primarily caused by energetic protons with kinetic energy more than a few keV. This is evidenced by the DMSP satellite detection of the electron and proton precipitation profiles across the diffuse auroral undulations (see Figure 1*c*). Note that the number fluxes, energy fluxes, and average energies of the precipitated protons (in the lower panel of Figure 1*c*) are enhanced only over that region.

The energetic particles causing the diffuse aurora execute gradient-B and curvature drifts in the azimuthal direction and change their drift velocities ($V_G + V_C$) during their field-aligned motion. As a first approximation in our two-dimensional model, we assume that energetic particles move in the ionospheric plane with the electric drift velocity (V_E) plus the virtual magnetic drift velocities $\langle V_{G+C,i} \rangle$ defined as follows. When the particle motion at an altitude of s is

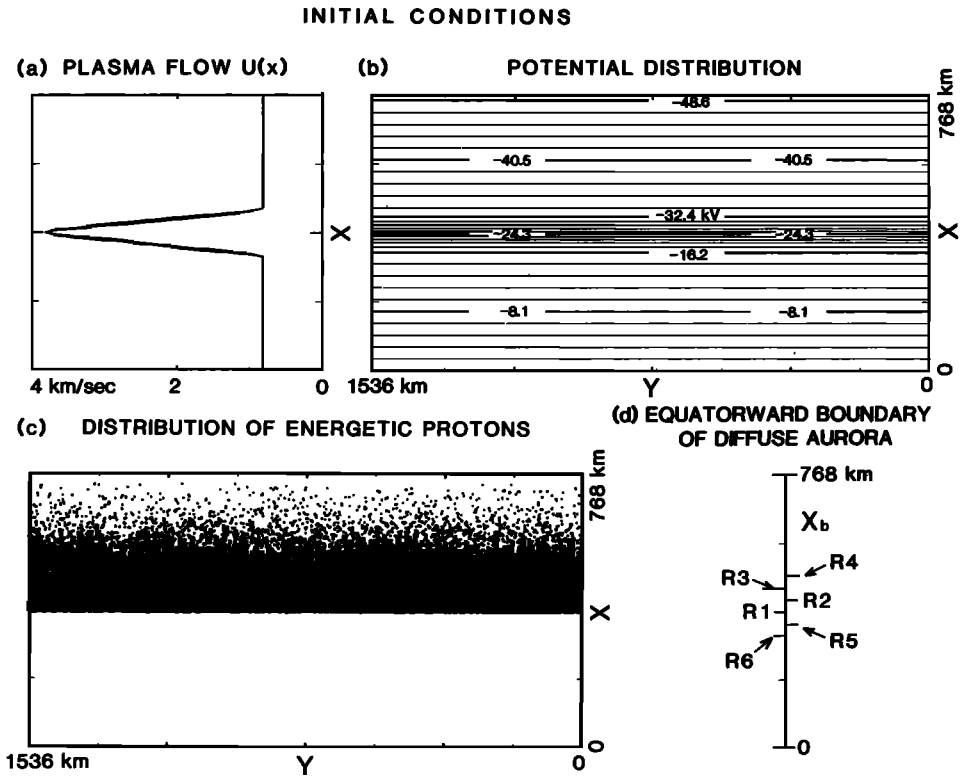

Fig. 3. Initial conditions for the simulations. (*a*) Westward flow $U(x)$ of a cold plasma. (*b*) Distribution of the electrostatic potential associated with the flow pattern $U(x)$. Potential values are in units of kilovolts. Contour intervals are 1.62 kV. (*c*) Spatial distribution of energetic protons in run 1. (*d*) Position x_b of the equatorward boundaries of the energetic proton clusters for runs 1–6.

projected, along a field line, onto the ionospheric plane, the projected value of a total magnetic drift velocity $V_{G+C} = V_G + V_C$ is given by

$$V_{G+C,i} = [B(s)/B_i]^{0.5} V_{G+C}(s)$$

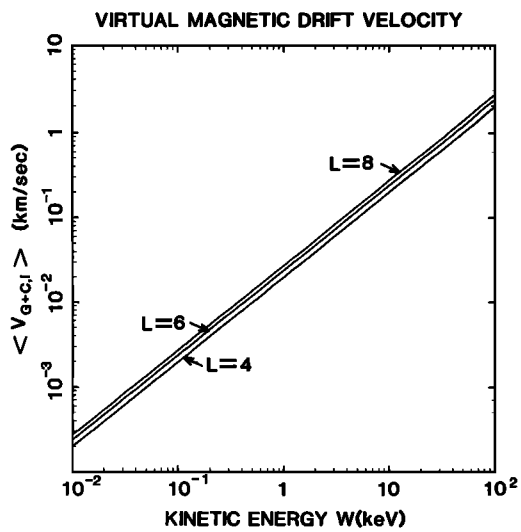

Fig. 4. Virtual magnetic drift velocities $\langle V_{G+C,i} \rangle$ (kilometers per second) (defined in the text) plotted as functions of the particle kinetic energy W (keV) for the Earth dipole field lines at various L values.

where $B(s)$ and B_i are the magnetic field intensities at the altitude s and at the ionospheric altitude on the field line, respectively. The projected velocity $V_{G+C,i}$ of a particle with total kinetic energy $W = W_\perp + W_\parallel$ and equatorial pitch angle α_e is averaged over its transit period from the equator to the ionosphere or the mirror point, and the value thus obtained is averaged over the pitch angle range of $0 \leq \alpha_e \leq 30°$. (Note that energetic particles with small pitch angles will primarily be responsible for the brightening of the diffuse aurora.) In this calculation, adiabatic motion of a particle and an isotropic distribution of the particle velocities are assumed. In Figure 4 the averaged values $\langle V_{G+C,i} \rangle$, which are called the virtual magnetic drift velocities in the ionospheric plane, are plotted as functions of W for the dipole field lines at various L values. In the present analysis the virtual magnetic drift velocities $\langle V_{G+C,i} \rangle(W)$ of energetic particles in the simulation plane are assumed constant (in time and space).

The diffuse aurora is thought to be caused by precipitation of energetic protons with energies W above a certain level W_c (approximately a few keV). (Such precipitation may be due to pitch angle scattering through wave-particle interactions.) Therefore, in our model, the two-dimensional evolution of the diffuse aurora is obtained by following the energetic protons that have virtual magnetic drift velocities greater than $\langle V_{G+C,i} \rangle(W_c)$. For simplicity the distribution of $\langle V_{G+C,i} \rangle$ is given by a truncated ($> \langle V_{G+C,i} \rangle(W_c)$) Gaussian with a most probable value V_P and standard deviation σ.

The initial spatial distribution of the diffuse auroral pro-

tons in run 1 is shown in Figure 3*c*. In runs 2–6, only the latitude of the equatorward boundary of the auroral proton cluster is changed. The boundary positions x_b for runs 1–6 are also indicated in Figure 3*d*.

Since protons and electrons of an energetic plasma magnetically drift in opposite directions, space charges tend to arise from density irregularities in the plasma. On the poleward boundary of the energetic plasma, charge separation can proceed further and deform the boundary in a similar way to the Rayleigh-Taylor instability. This instability has been proposed as the mechanism for the generation of auroral omega bands by T. Yamamoto et al. (A particle simulation of auroral omega bands and torchlike structures, submitted to *Journal of Geophysical Research*, 1990). In this sense, the equatorward boundary of the energetic plasma is quite stable, as is shown by their numerical simulation. It can then be understood that the above mentioned instability arising from charge separation in an energetic plasma has nothing to do with the deformation of the equatorward boundary of the energetic plasma. To more closely examine possible effects of charge separation in the energetic plasma, we perform two additional test runs in addition to the main simulation runs. In the tests we assume the same initial distribution of cold particles as in the main runs, and we use the same boundary conditions (stated below). The initial distributions of energetic particles are again specified as shown in Figure 3*c*, and the proton and electron distributions are initially the same so that the energetic plasma is neutral. To suppress the Rayleigh-Taylor-type instability on the poleward boundary of the energetic plasma, we assume that the density gradient on this side is small. The energy distribution of the energetic protons is essentially the same as in the main runs. For simplicity, magnetic drifts of the electrons are neglected. In test 1, space charges from the energetic plasma are self-consistently treated under the condition that the energetic plasma density is smaller than that of the nonuniform part of a cold plasma. In test 2, space charges from the energetic plasma are neglected in calculating the potential distribution at each time step. In these tests, K-H waves are driven by the velocity shear of the cold plasma flow, and associated modulations of the energetic plasma occur. Similar large-scale patterns of the modulations are observed in both test runs. In test 1, random fluctuations on a small scale (approximately a few tens of kilometers) are seen in the energetic plasma density and the potential distribution. Since small-scale fluctuations are not observed in test 2, the generation of such fluctuations is attributed to charge separation in the energetic plasma. (It may be suggested that this phenomenon is related to the patchy structure observed in the diffuse aurora region [e.g., *Oguti*, 1981].) Since the aim of our simulation is to study the large-scale deformation of the equatorward boundary of the diffuse aurora, we are allowed to neglect space charges in the energetic plasma. Thus, in the present model, the diffuse auroral protons are treated as "test particles."

The particle simulations are performed by using a particle-in-cell code [e.g., *Okuda*, 1985]. Our two-dimensional computational mesh size is $N_x \times N_y = 128 \times 256$. The grid spacing Δ is then $L_x/128 = L_y/256 = 6$ km. In a two-dimensional guiding center model, Δ is not required to be less than the proton Larmor radius nor the Debye length. For the strips of cold particles producing the sheared flow, 20,480 particles are used. Initially, they are uniformly loaded in the strips, and the number density per cell is 4. Since the background uniform plasma is assumed to be neutral, there is no need to load particles for this particle population. The number of particles used for the auroral protons is about 20,000. The results to be presented are from runs using a time step at $\Delta t = 1.0$ s. The time step Δt is taken small enough to satisfy the Courant condition of $V_m \Delta t < \Delta$, where V_m is the maximum particle speed. The guiding center positions of particles are advanced by using the predictor-corrector method [*Lee and Okuda*, 1978]. The Poisson's equation is solved by using the standard five-point finite difference approximation. The boundary conditions on the potential are periodic in the longitudinal (y) direction and bounded in the latitudinal (x) direction. On the boundaries at $x = 0$ and $x = L_x$ the longitudinal flow speeds V_E are fixed at the initial value of V_E (see Figure 3*a*). The boundary conditions on particles are periodic in both the x and y directions. In the actual simulation runs, no cold particles pass the boundary at $x = 0$ (or L_x), and very few auroral protons pass it. In test runs it was found that the temporal evolution of the electrostatic Kelvin-Helmholtz instability is not significantly changed by increasing the number of particles per cell (in the strips) from 4 to 8, nor by decreasing the time step Δt from 1.0 s to 0.5 s.

4. Simulation Results

In this section we show how the spatial distribution of the diffuse auroral protons is modified by the Kelvin-Helmholtz instability developing from the plasma flow pattern specified in Figures 3*a* and 3*b*. As for the distribution of the virtual magnetic drift speed $\langle V_{G+C,i} \rangle$ of the auroral protons, we choose the parameters as the most probable value $V_P = 0.19$ km/s, the standard deviation $\sigma = 0.13$ km/s, and the minimum speed $\langle V_{G+C,i} \rangle (W_c) = 0.076$ km/s. From Figure 4 it is found that protons with magnetic drifts of 0.19 and 0.076 km/s have total kinetic energies of about 8 and 3 keV, respectively, when the magnetic shell at $L \sim 5$ is considered. Recall that the average energy of the precipitating protons can exceed 10 keV over the diffuse aurora as seen in Figure 1*b*. By performing runs 1–6 we examine how the undulation pattern of the diffuse aurora is changed with the latitude of the auroral boundary relative to the zone of the enhanced plasma flow.

Figures 5–7 are the results from run 1, in which the initial distribution of the diffuse aurora is given as shown in Figure 3*c* (the boundary position x_b is $L_x/2$). Figure 5*a* shows the temporal evolution of the electrostatic potential distribution, or, equivalently, the streamlines associated with $E \times B$ drift. The potential ϕ in Figure 5*b* is calculated by imposing the condition that $\partial\phi/\partial x = 0$ on the boundaries at $x = 0$ and $x = L_x$. Thus the potential ϕ in Figure 5*b* is primarily formed from space charges inside the simulation domain. On the other hand, the potential in Figure 5*a* is calculated under the condition that the longitudinal flow speeds at $x = 0$ and L_x are fixed at the initial value of V_E (see Figure 3*a*). As a consequence, this potential includes a uniform (inside the domain) meridional electric field due to outer space charges. (Note that initially, the meridional electric field on the boundaries at $x = 0$ and $x = L_x$ is entirely due to space charges outside the simulation domain. This is so because the total amount of space charges inside the simulation domain is zero and the initial particle distribution is uniform

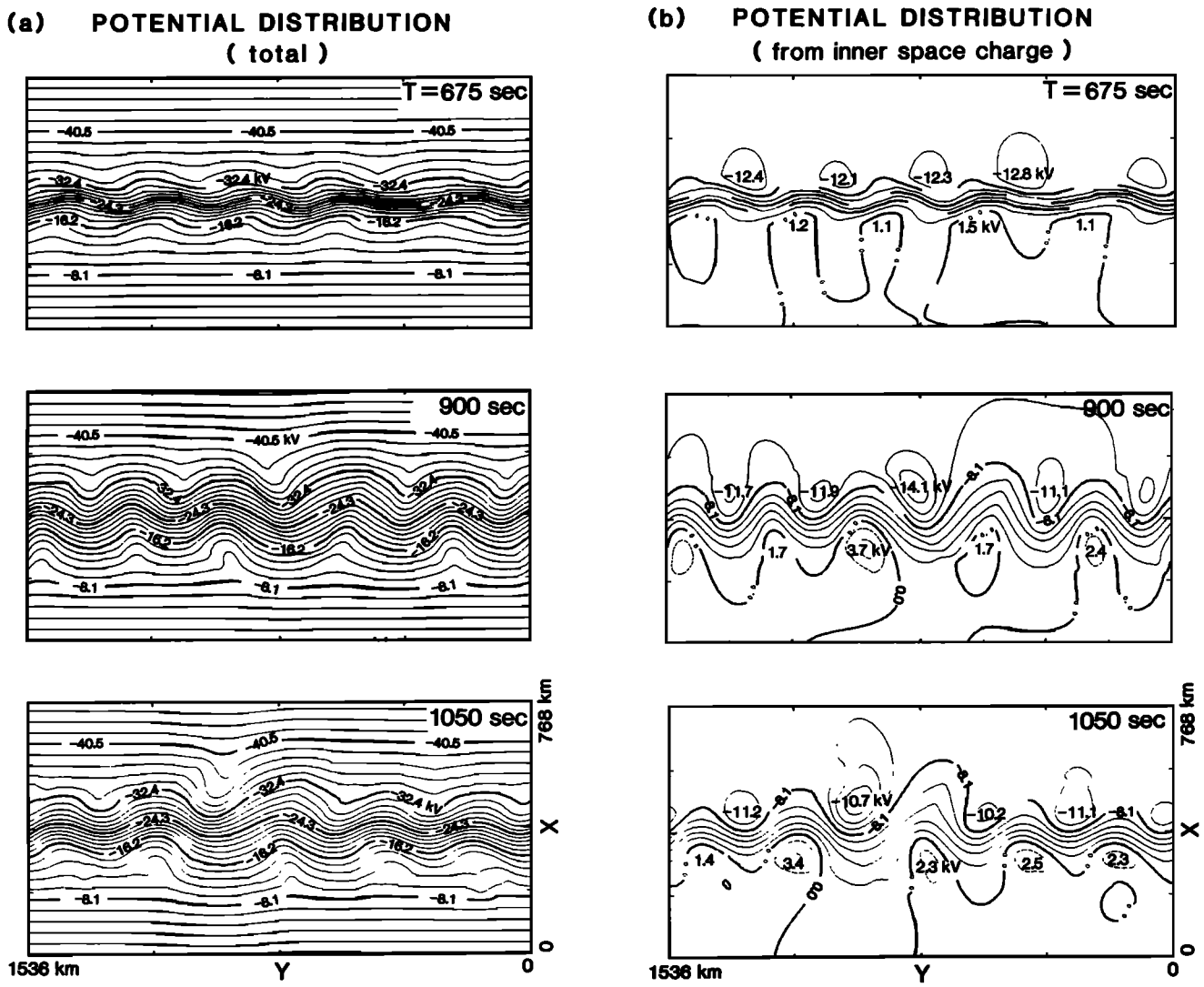

Fig. 5. (*a*) Temporal evolution of the electrostatic potential distribution. (*b*) Potential (ϕ) distributions (arising from space charges inside the simulation domain) at the same times as in Figure 5*a*, which are calculated by imposing the condition of $\partial\phi/\partial x = 0$ on the boundaries at $x = 0$ and $x = L_x$. Potential distributions in Figures 5*a* and 5*b* are common to all runs. Potential values are in units of kilovolts and contour intervals are 1.62 kV.

in y. In the later period, since space charges from the cold particle strips are still confined in a small latitudinal dimension, the electric field of internal origin is negligible near the boundaries at $x = 0$ and L_x.) Thus the $E \times B$ can be considered as a combination of the background (uniform) westward flow due to outer space charges and the perturbed flow due to inner space charges. The streamlines of the perturbed flow are shown in Figure 5*b*. Figure 6 shows the temporal evolution of the spatial distribution of the energetic protons, which is identified with the temporal evolution of the diffuse auroral pattern. To understand the significance of the magnetic drifts of the energetic protons for the formation of undulations on the diffuse auroral boundary, we also follow the test particles without magnetic drifts, which have initially the same distribution as the energetic protons, and compare the two distributions. Figure 7 shows the distribution of the particles without magnetic drifts at $t = 900$ s, when the diffuse auroral undulations are fully developed as seen in Figure 6.

As seen from Figure 5*b*, two lines of vortices are developed on both sides of the streamlines for the most intense westward flow. Accumulation of positive charges is centered around each vortex on the equatorward line while negative charge accumulation is on the poleward line. "Staggered" formation of vortices of oppositely charged polarities, such as that seen in Figure 5*b*, has been studied, for example, by *Yamamoto and Yamashita* [1988]. Note that a vortex cell is only barely formed in the streamlines in Figure 5*a* due to addition of the uniform westward flow.

According to the linear analysis of the electrostatic K-H instability for the flow velocity profile of U_m sech^2 (x/L) [*Ganguli et al.*, 1988], the temporal growth rate γ_m and the wavelength λ_m of the most unstable mode are estimated as

$$\lambda_m = 7.0L \qquad \gamma_m = 0.16U_m/L \tag{3}$$

where U_m is the maximum flow speed and L is the shear scale in the velocity profile. Although the initial profile of the flow velocity in the present simulations is different from that assumed by Ganguli et al., substitution of $L \approx 7\Delta = 42$ km and $U_m \approx 3.8$ (at $x = L_x/2$) $- 0.81$ (at $x = 0$) $= 3.0$ km/s into

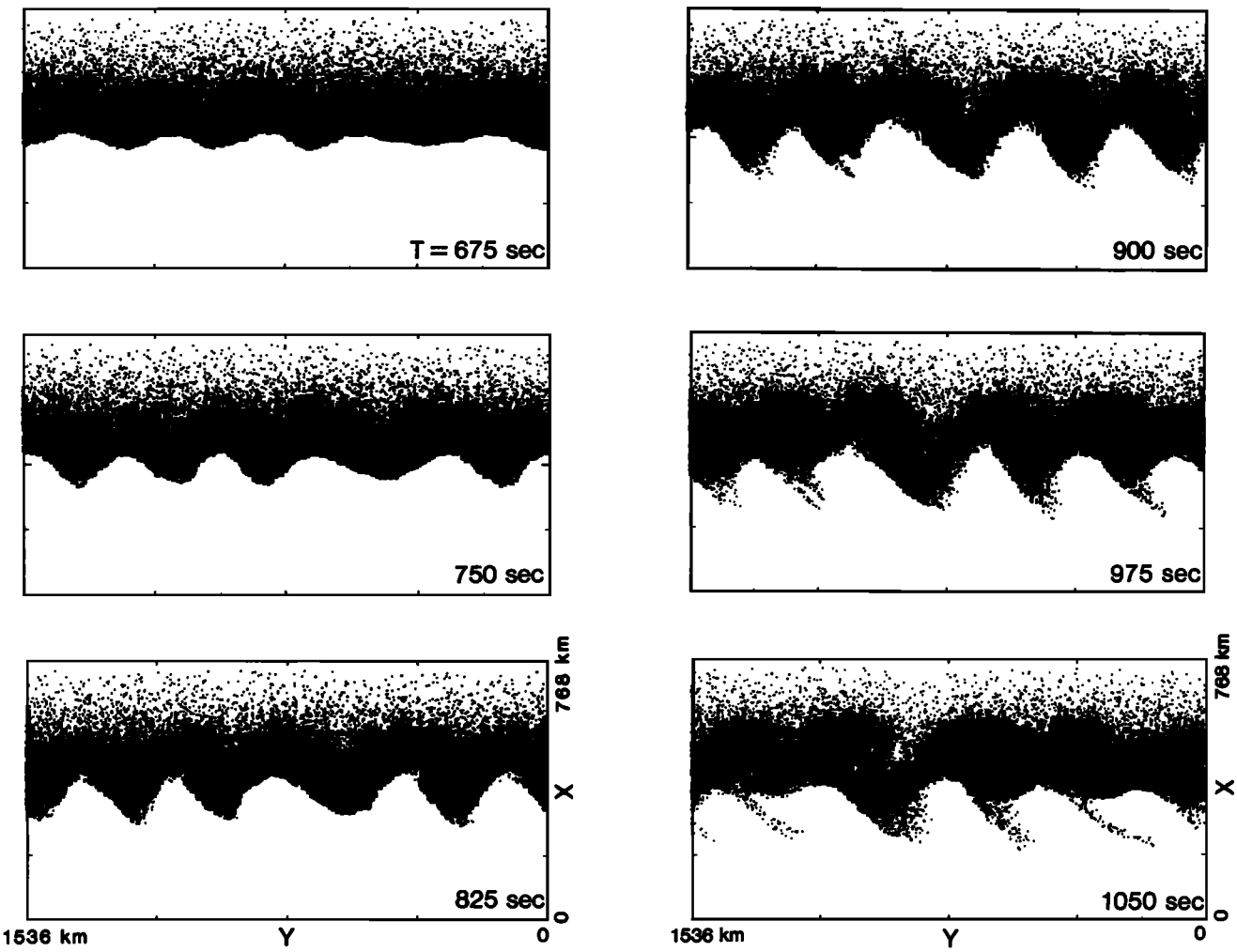

Fig. 6. Temporal evolution of the spatial distribution of the energetic protons (diffuse auroral pattern), for run 1.

(3) yields a rough estimation of $\gamma_m^{-1} \approx 88$ s and $\lambda_m \approx 290$ km. Actually, the wavelengths of the undulations in our simulations are about $50\Delta = 300$ km, which is the typical wavelength of the observed undulations. The apparent phase velocity of the undulations is found to be ~1.6 km/s, which is expected to be about the average westward speed of the plasma flow around the vortices.

In discussing the modulation of the diffuse auroral boundary, the time t_d required for the development of a vortex, defined as follows, is more practical than the growth time defined by γ^{-1}. The developing time t_d is defined by a period during which the maximum radius of nearly circular (closed) streamlines associated with a developing vortex increases by the length of a shear scale. The time t_d in our simulations is about 700 s, which is even longer than the growth time. A vortex travels over the distance of $V_0 t_d$ before that vortex causes a significant modulation on the diffuse auroral boundary, where V_0 is the average westward velocity of the plasma

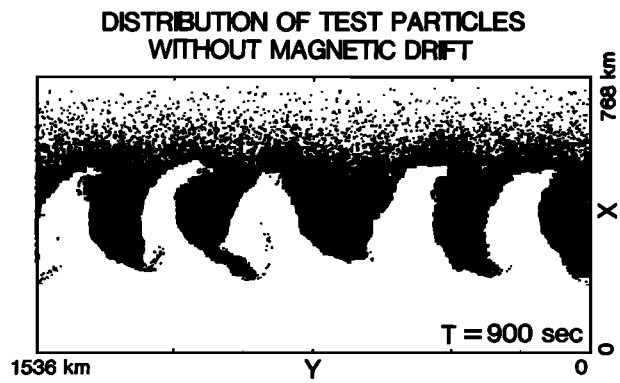

Fig. 7. Distribution of test particles without magnetic drifts at $t = 900$ s. The initial distribution of these particles is the same as that of the energetic protons in run 1.

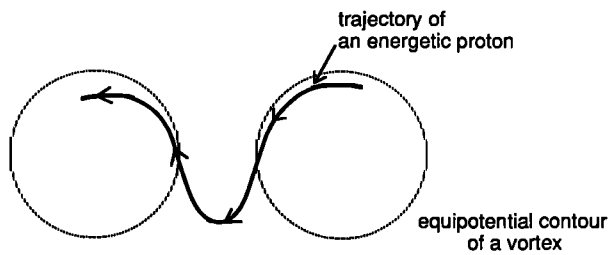

Fig. 8. Schematic illustrating a trajectory of an energetic proton in the presence of a chain of vortices. The westward magnetic drift of an energetic proton can act to prevent it from being trapped in the vortices.

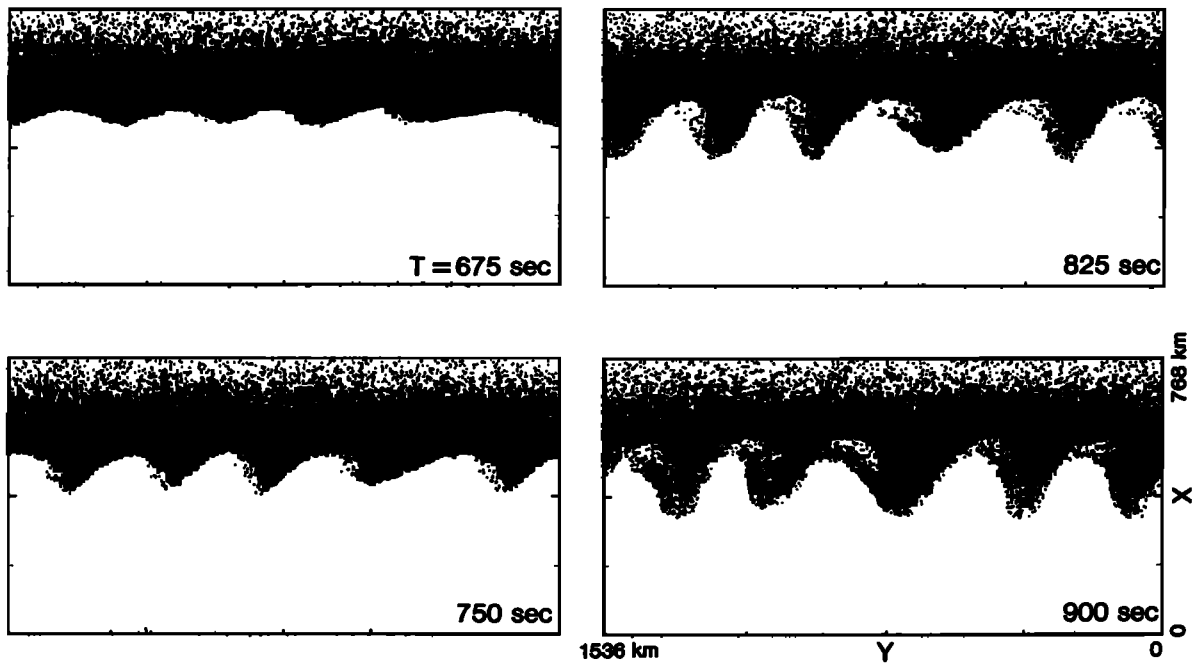

Fig. 9. Same format as Figure 6 but for run 4.

flow around the vortex. Therefore the distance V_0t_d will be required to be small enough for the emergence of large-amplitude undulations on the diffuse auroral boundary. From the simulation result, V_0t_d is estimated as $V_0t_d \approx 1100$ km, which is short enough in comparison with the longitudinal length of a diffuse aurora.

It can easily be understood how indentations such as those shown in Figure 6 develop on the diffuse auroral boundary located around the region of the most intense westward flow. The background westward flow, i.e., the $E \times B$ drift due to the uniform poleward electric field, does not contribute to the undulation of the diffuse auroral boundary. The motion of a particle relative to the background flow is due to the $E \times B$ drift in the electric field from inner space charges and the magnetic drift. Some protons are incorporated into growing vortices, i.e., start the circular motion of the $E \times B$ drift, following the closed streamlines in Figure 5*b*. These protons are forming the peninsulas extending equatorward. If the particle energy is small so that the magnetic drift is negligible, the particle completes the circular motion. This behavior of cold particles characterizes the distribution of the test particles without magnetic drifts as shown in Figure 7. On the other hand, when energetic protons are nearly trapped in a vortex, they can escape from the circular streamlines associ-

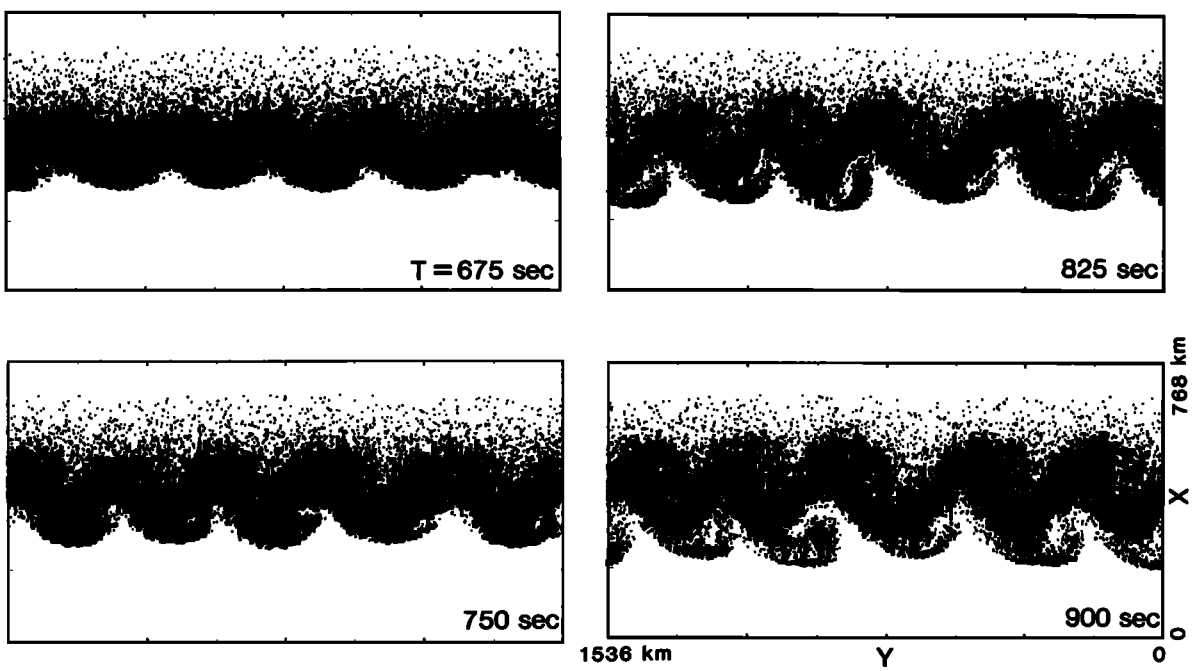

Fig. 10. Same format as Figure 6 but for run 6.

ated with that vortex because of their magnetic drifts. A physical trajectory of an energetic proton is schemetically shown in Figure 8. It is understood that the cluster of the diffuse auroral protons can form the equatorward extending peninsulas, when it is modulated by the K-H waves.

From the above considerations the undulation pattern is expected to vary depending on the location (x_b) of the diffuse auroral boundary relative to the zone of the enhanced plasma flow (see the boundary positions x_b for runs 1–6 in Figure 3*d*). The temporal evolutions of the spatial distributions of the auroral protons in runs 4 and 6 are shown in Figures 9 and 10, respectively. In runs 2–5 it is found that large-amplitude undulations with a similar pattern can finally develop on the equatorward boundary of the diffuse aurora. In run 6 the energetic protons on the boundary are trapped in the central parts of the vortices developing at low altitudes. The spiraling structure appears on the boundary. In runs 3 and 4 the same kind of dynamics can act on protons near the boundary because the auroral boundaries are initially set so as to cross the central parts of the developing vortices at high latitudes. In these cases, the magnetic drifts blow off, westward, some protons that are nearly trapped in the vortices with a clockwise rotation as if water waves were broken off by a strong wind. This phenomenon is seen at t = 750 and 825 s in run 4 (Figure 9). Subsequently, the blown-off protons merge into the main body of the proton cluster. Eventually, the same large-scale patterns of undulations as in run 1 are formed, although small gaps in the proton cluster still remain.

Finally, we need to point out that our two-dimensional simulation model does not include effects of field-aligned currents and associated magnetosphere-ionosphere coupling. Recent numerical simulations have shown that effects of Pedersen conductivity of the F layer can reduce the growth rate of the Kelvin-Helmholtz instability and inhibit vortex formation [*Keskinen et al.*, 1988]. They have considered such Pedersen coupling effects, assuming that the height-integrated density of the F layer is proportional to that of a magnetospheric region with polarization currents. Consequently, their results may not be applied directly to the diffuse auroral phenomenon studied here, in which the ionospheric plasma density is locally influenced by precipitation of energetic particles. Inclusion of ionospheric coupling effects in particle simulations will be the next step of our study of auroral dynamics.

5. Conclusions

Using two-dimensional particle simulations, we have shown that large-amplitude undulations observed on the equatorward boundary of the proton diffuse aurora can be identified with spatial modulations of the distribution of energetic protons by Kelvin-Helmholtz waves. In our model, the temporal evolution of the diffuse auroral pattern is obtained by following in time the positions of the energetic protons projected onto the ionospheric plane. Chains of vortices are generated by the K-H instability from local (in latitude) enhancement of the westward convection flow, which is consistent with the observed distributions of the electric fields or plasma flow velocities. These vortices can spatially modulate the cluster of energetic protons, which results in the undulation patterns of the auroral boundaries similar to those observed. It should be emphasized that the magnetic drifts of the auroral protons greatly contribute to creation of the characteristic undulation pattern.

Acknowledgments. One of the authors (T.Y.) would like to thank N. Hori for performing numerical experiments to find a plausible model of the diffuse auroral ripple, and E. Kaneda and A. Miura for useful discussions. The authors are grateful to S.-I. Akasofu for providing the valuable satellite data on auroral images and particle precipitation. T.Y. also would like to thank the Editor for helpful suggestions.

The Editor thanks two referees for their assistance in evaluating this paper.

References

Ganguli, G., Y. C. Lee, and P. J. Palmadesso, Kinetic theory for electrostatic waves due to transverse velocity shears, *Phys. Fluids*, *31*, 823, 1988.

Gonzales, C. A., M. C. Kelley, R. A. Behnke, J. F. Vickrey, R. Wand, and J. Holt, On the latitudinal variations of the ionospheric electric field during magnetospheric disturbances, *J. Geophys. Res.*, *88*, 9135, 1983.

Hallinan, T. J., and T. N. Davis, Small scale auroral arc distortions, *Planet. Space Sci.*, *18*, 1735, 1970.

Kelley, M. C., Intense sheared flow as the origin of large-scale undulations of the edge of the diffuse aurora, *J. Geophys. Res.*, *91*, 3225, 1986.

Keskinen, M. J., H. G. Mitchell, J. A. Fedder, P. Satyanarayana, S. T. Zalesak, and J. D. Huba, Nonlinear evolution of the Kelvin-Helmholtz instability in the high-latitude ionosphere, *J. Geophys. Res.*, *93*, 137, 1988.

Lee, W. W., and H. Okuda, A simulation model for studying low frequency micro instabilities, *J. Comput. Phys.*, *26*, 139, 1978.

Lui, A. T. Y., C.-I. Meng, and S. Ismail, Large amplitude undulations on the equatorward boundary of the diffuse aurora, *J. Geophys. Res.*, *87*, 2385, 1982.

Lyons, L. R., and R. L. Walterscheid, Generation of auroral omega bands by shear instability of the neutral winds, *J. Geophys. Res.*, *90*, 12,321, 1985.

Maynard, N. C., On large poleward-directed electric fields at subauroral latitudes, *Geophys. Res. Lett.*, *5*, 617, 1978.

Miura, A., and T. Sato, Shear instability: Auroral arc deformation and anomalous momentum transport, *J. Geophys. Res.*, *83*, 2109, 1978.

Nishikawa, K.-I., G. Ganguli, Y. C. Lee, and P. J. Palmadesso, Simulation of ion-cyclotron-like modes in a magnetoplasma with transverse inhomogeneous electric field, *Phys. Fluids*, *31*, 1568, 1988.

Oguti, T., Rotational deformations and related drift motions of auroral arcs, *J. Geophys. Res.*, *79*, 3861, 1974.

Oguti, T., TV observations of auroral arcs, in *Physics of Auroral Arc Formation*, *Geophys. Monogr. Ser.*, vol. 25, edited by S.-I. Akasofu and J. R. Kan, p. 31, AGU, Washington, D. C., 1981.

Okuda, H., Introduction to particle simulation models and other application to electrostatic plasma waves, in *Computer Simulation of Space Plasmas*, vol. 3, p. 3, edited by H. Matsumoto and T. Sato, Terra Scientific, Tokyo, 1985.

Pritchett, P. L., Electrostatic Kelvin-Helmholtz instability produced by a localized electric field perpendicular to an external magnetic field, *Phys. Fluids*, *30*, 272, 1987.

Pritchett, P. L., and F. V. Coroniti, The collisionless macroscopic Kelvin-Helmholtz instability, 1, Transverse electrostatic mode, *J. Geophys. Res.*, *89*, 168, 1984.

Rich, F. J., W. J. Burke, M. C. Kelley, and M. Smiddy, Observations of field-aligned currents in association with strong convection electric fields at subauroral latitudes, *J. Geophys. Res.*, *85*, 2335, 1980.

Satyanarayana, P., Y. C. Lee, and J. D. Huba, Transverse Kelvin-Helmholtz instability with parallel electron dynamics and Coulomb collisions, *J. Geophys. Res.*, *92*, 8813, 1987.

Smiddy, M., M. C. Kelley, W. Burke, R. Rich, R. Sagalyn, B. Shuman, R. Hays, and S. Lai, Intense poleward-directed electric fields near the ionospheric projection of the plasmapause, *Geophys. Res. Lett.*, *4*, 543, 1977.

Spiro, R. W., R. A. Heelis, and W. B. Hanson, Rapid subauroral ion drifts observed by Atomospheric Explorer C, *Geophys. Res. Lett.*, *6*, 657, 1979.

Unwin, R. S., and C. H. Cummack, Drift spikes: The ionospheric signature of large poleward directed electric fields at subauroral latitudes, *Planet. Space Sci.*, *28*, 72, 1980.

Viñas, A. F., and T. R. Madden, Shear flow-ballooning instability as a possible mechanism for hydromagnetic fluctuations, *J. Geophys. Res.*, *91*, 1519, 1986.

Wagner, J. S., R. D. Sydora, T. Tajima, T. Halliman, L. C. Lee, and S.-I. Akasofu, Small-scale auroral arc deformations, *J. Geophys. Res.*, *88*, 8013, 1983.

Yamamoto, T., and M. A. Yamashita, Convective generation of a vortex street in plasma shear flow, *Phys. Fluids*, *31*, 2152, 1988.

K. Makita, Takushoku University, Hachioji, Tokyo 193, Japan.

C.-I. Meng, Applied Physics Laboratory, Johns Hopkins Road, Laurel, MD 20707.

T. Yamamoto, University of Tokyo, Bunkyo-ku, Tokyo 113, Japan.

(Received September 25, 1989;
revised July 16, 1990;
accepted August 16, 1990.)